Variable Temperature X-ray Crystal Structure Analysis of a Type I Langbeinite: $Rb_2Cd_2(SO_4)_3$

G. Nalini and T. N. Guru Row*

Solid State and Structural Chemistry Unit, Indian Institute of Science, Bangalore 560 012, India

Received May 13, 2002. Revised Manuscript Received July 23, 2002

The structure of a type I langbeinite, $Rb_2Cd_2(SO_4)_3$, displays three different phases, cubic with $a = 10.378(5)$ Å (space group $P2_13$) at room temperature, monoclinic at 120 K with $a = 10.328(3)$, $b = 10.322(3)$, $c = 10.325(3)$ Å, $\beta = 89.975(1)°$ (space group $P2_1$), and orthorhombic at 85 K with $a = 10.319(2)$, $b = 10.321(2)$, $c = 10.320(2)$ Å (space group $P2_12_12_1$), respectively. Precise single-crystal analyses of these phases indicate that $Rb_2Cd_2(SO_4)_3$ distorts initially from cubic to monoclinic upon cooling followed by a significant reorientation of the SO_4 tetrahedra, resulting in an orthorhombic symmetry upon further cooling. The three structures have been established unequivocally using the same crystal. There is no indication of the formation of an intermediate triclinic phase or any lattice disorder as conjectured in several earlier reports on compounds belonging to the type I langbeinite. The bond valence sum analyses of the coordination around the Rb sites indicate asymmetry in the bond strengths which could be the driving force of the ferroelectric behavior in these materials.

Introduction

The langbeinite family of sulfates with the general formula $A_2B_2(SO_4)_3$ with A = K, NH_4, Tl, Rb, Cs and B = Mn, Cd, Co, Ca represents a class of ferroelastic and ferroelectric materials.[1] X-ray diffraction studies have shown that crystals of these materials have a cubic structure with space group $P2_13$ at room temperature with a lattice parameter of nearly 10 Å and four formula units per unit cell. Theoretical calculations by Dvora'k[2,3] suggest that these crystals can transform to low-temperature phases with several possible space groups: $P2_1$, $R3$, $P1$, and $P2_12_12_1$. So far in the literature there have been two different sequences of phase transition identified; one with cubic → orthorhombic distortion and the other with cubic → monoclinic → triclinic → orthorhombic distortion.[4] Compounds $K_2Cd_2(SO_4)_3$ and $K_2Mn_2(SO_4)_3$ show, for example, only a single-phase transition and are grouped as type II langbeinites.[5,6] Several type II structures have been analyzed by single-crystal X-ray diffraction,[7,8] and the mechanism of phase transition has been attributed to the simultaneous translation and rotation of the SO_4 group and the subsequent rearrangement in the B^{2+} and A^{1+} cation positions.[9,10]

The langbeinites that show multiple phase transitions such as $Tl_2Cd_2(SO_4)_3$ (hereafter TlCdS) and $Rb_2Cd_2(SO_4)_3$ (hereafter RbCdS) are classified as type I compounds.[4] It is of interest to note that so far there is only one detailed single-crystal X-ray diffraction study followed by a subsequent phase transition analysis in the literature.[11,12] The phase transition mechanism in $K_2Co_2(SO_4)_3$ and $K_2Zn_2(SO_4)_3$[13,14] were earlier explained in terms of an order−disorder mechanism in the cubic phase triggered at the nucleation site during crystallization. The structure of TlCdS has been shown to differ very little from the high-temperature cubic structure, and the resulting monoclinic phase further proceeds to the orthorhombic symmetry via a metastable triclinic phase.[12] The subtle interplay between the monoclinic and the triclinic phases has been discussed in detail in terms of possible transformation matrixes. However, the single-crystal X-ray diffraction at 121 K indicates that the monoclinic structure may be disordered. The goodness of fit of the refined structure is rather large ($S = 13.75$) while the corresponding precession photographs do not display appreciable deviation from the monoclinic symmetry.[12] The conclusions drawn from this study point out that the rotations of the SO_4 groups together with small displacement of heavy atoms seem to be the most important factor driving the phase transition.

* To whom correspondence should be addressed. Fax: +91-80-3601310. E-mail: ssctng@sscu.iisc.ernet.in.

(1) Zemann, A.; Zemann, J. *Acta Crystallogr.* **1957**, *10*, 409.
(2) Dvorak, V. *Phys. Status Solidi B* **1972**, *52*, 93.
(3) . Dvorak, V. *Phys. Status Solidi B* **1974**, *66*, K87.
(4) Yamada, N.; Maeda, M.; Hideaki, A. *J. Phys. Soc. Jpn.* **1981**, *50*, 907.
(5) Abrahams, S. C.; Lissalde, F.; Bernstein, J. L. *J. Chem. Phys.* **1978**, *68*, 1926.
(6) Brezina, B.; Glogarov, M. *Phys. Status Solidi A* **1972**, *11*, K39.
(7) Abrahams, S.; Bernstein, J. L. *J. Chem. Phys.* **1977**, *67*, 2146.
(8) Ukeda, U.; Kazuyuki, I.; Moriyoshi, C. *J. Phys. Soc. Jpn.* **1995**, *64* (2), 504.
(9) Lissalde, F.; Abrahams, S. C.; Bernstein, J. L.; Nassau, K. *J. Appl. Phys.* **1979**, *50*, 845.
(10) Guelylah, A.; Aroyo, M. I.; Perez-Mato, J. M. *Phase Transitions* **1996**, *59*, 155.
(11) Guelylah, A.; Madariaga, G.; Breczewski, T. *Acta Crystallogr.* **1996**, *C52*, 2954.
(12) Guelylah, A.; Madariaga, G.; Morgenroth, W.; Aroyo, M. I.; Breczewski, T.; Bocanergra, E. H. *Acta Crystallogr.* **2000**, *56*, 921.
(13) Moriyoshi, C.; Itoh, K.; Tomoyuki, H. *J. Phys. Soc. Jpn.* **1995**, *64* (12), 4726.
(14) Moriyoshi, C.; Itoh, K. *J. Phys. Soc. Jpn.* **1996**, *65* (11), 3537.

10.1021/cm020566h CCC: $22.00
Published on Web 08/30/2002

Table 1. Crystal Data, Measurement, and Structure Refinement Parameters for $Rb_2Cd_2(SO_4)_3$

empirical formula	$Rb_2Cd_2(SO_4)_3$	$Rb_2Cd_2(SO_4)_3$	$Rb_2Cd_2(SO_4)_3$
crystal color	colorless[a]	colorless[a]	colorless[a]
crystal size (mm)	0.3 × 0.2 × 0.04	0.3 × 0.2 × 0.04	0.3 × 0.2 × 0.04
crystal system	cubic	monoclinic	orthorhombic
space group	$P2_13$	$P2_1$	$P2_12_12_1$
cell dimensions (Å/deg)	$a = 10.378(5)$	$a = 10.328(3)$	$a = 10.319(2)$
		$b = 10.322(3)$	$b = 10.321(2)$
		$c = 10.325(3)$	$c = 10.320(2)$
		$\beta = 89.975(1)$	
volume (Å^3)	1117.56(5)	1100.64(1)	1099.10(4)
formula weight	623.98	623.98	623.98
density (calcd)g/cm^3	4.06	4.13	4.13
Z	4	4	4
F(000)	1255.8	1255.8	1255.8
	Data Collection		
equipment	Bruker axs SMART APEX CCD	Bruker axs SMART APEX CCD	Bruker axs SMART APEX CCD
λ (Mo Kα (graphite monochromator)) (Å)	0.7107	0.7107	0.7107
scan mode	ω scan	ω scan	ω scan
temperature (K)	298	120	85
θ range (deg)	2.8−27.9°	2−27.5°	2.8−23.2°
recording reciprocal space	$-13 \rightarrow h \rightarrow 13$	$-13 \rightarrow h \rightarrow 13$	$-11 \rightarrow h \rightarrow 11$
	$-13 \rightarrow k \rightarrow 13$	$-13 \rightarrow k \rightarrow 13$	$-11 \rightarrow k \rightarrow 11$
	$-13 \rightarrow l \rightarrow 13$	$-13 \rightarrow l \rightarrow 13$	$-11 \rightarrow l \rightarrow 11$
no. of measured reflections	15896	12743	11518
no. of independent reflections	907	4998	1587.
μ (mm^{-1})	13.3	13.3	13.3
Flack parameter	−0.029(14)	0.017(7)	0.019(11)
data reduction	SAINT PLUS	SAINT PLUS	SAINT PLUS
absorption correction	SADABS	SADABS	SADABS
	Refinement		
no. of refined parameters	59	344	172
refinement method	full matrix least squares	full matrix least squares	full matrix least squares
$R[I > 4\sigma I]/R$[all data]	0.029/0.028	0.035/0.038	0.026/0.027
wR $[I > 4\sigma I]/R$[all data]	0.069/0.07	0.083/0.082	0.061/0.061
GoF	1.09	1.04	1.09
max/min $\Delta\rho$ eÅ^{-3}	0.58/−0.98	1.15/−0.95	0.9/−0.78

[a] The same crystal is used for all three data sets.

Indeed, the sense of rotation of the tetrahedra in TlCdS is opposite to that observed in type II compounds with reduced rotation amplitudes. However, the studies related to TlCdS are subject to some concern as the existence of the intermediate triclinic phase remains an enigma. Studies of $K_2Zn_2(SO_4)_3$ and $K_2Co_2(SO_4)_3$,[13,14] on the other hand, clearly substantiate the absence of an intermediate triclinic phase. Thus, it appears that the phase transitions in type I langbeinites need a closer look.

The studies related to phase transition in RbCdS were limited to mapping changes in lattice parameters with temperature[15] and to studying the corresponding ferroelectric phase transition.[16] It is obvious from these studies that though the phase transition definitely goes through an intermediate monoclinic phase to the orthorhombic phase, there is no clear indication of the existence of another intermediate triclinic phase. We describe here a variable temperature single-crystal X-ray diffraction study of RbCdS at three different temperatures: the room-temperature cubic $P2_13$ phase, monoclinic phase at 120 K, and the orthorhombic phase at 85 K, respectively. Earlier phase transition studies[16] indicate the onset of the monoclinic phase is at 129 K and that of the orthorhombic phase is at 103 K. Our efforts were to evaluate the monoclinic phase precisely and to investigate the formation of any intermediate triclinic phase and thus the data were collected at 120 K. The orthorhombic phase has been analyzed likewise at 85 K. All of the three data sets have been collected on the same crystal.

Experimental Section

Single crystals of RbCdS were grown by evaporation at 358 K from an aqueous solution containing stoichiometric amounts, 1:2, of Rb_2SO_4 and $CdSO_4$. Beakers containing the solution (5 mL) were tightly corked to slow the evaporation rate at this temperature. The crystals obtained were transparent and colorless and were of good optical quality as tested under a polarizing microscope. The composition of the crystals was confirmed by preliminary powder X-ray diffraction as well as by EDAX measurements. DSC measurements (differential scanning calorimetry) in the temperature range 105 K to room temperature clearly brings out the signature for the change from cubic to monoclinic phase at 127 K. Further cooling to investigate the formation of the orthorhombic phase at 103 K could not be performed on the Perkin-Elmer DSC 2 system due to condensation and leakage. Variable temperature powder X-ray diffraction measurements have been performed on a STOE STADI-P diffractometer in the range 298−110 K at intervals of 10 K with an Oxford Cryosystem Nitrogen open-flow cryostat which provides a temperature stability of ±0.05 K.

(a) Structure at 298 K (Cubic $P2_13$ Case). A crystal of size 0.3 × 0.2 × 0.04 mm with sharp optical extinction was mounted on a BRUKER AXS SMART APEX CCD[17] diffracto-

(15) Yamada, N.; Shoichi, K. *J. Phys. Soc. Jpn.* **1977**, *43* (3), 1016.
(16) Hikita, T.; Kudo, T.; Chubachi, Y.; Ikeda, T. *J. Phys. Soc. Jpn.* **1976**, *41*, 349.

Table 2. Fractional Atomic Coordinates and Equivalent Thermal Parameters (U_{eq}): $U_{eq} = -(2\pi^2(U_{11}(ha^*))^2 + (U_{22}(kb^*))^2 + (U_{33}(lc^*))^2 + 2U_{12}hka^*b^* + 2U_{12}hla^*c^* + 2U_{23}klb^*c^*)$

atom	*x*	*y*	*z*	U_{eq} (Å)^2
		(a) 298 K		
Cd(1)	0.1680(1)	0.1680(1)	0.1680(1)	0.0135(2)
Cd(2)	0.4118(1)	0.4118(1)	0.4118(1)	0.0134(2)
Rb(1)	−0.1850(1)	0.3150(1)	0.1850(1)	0.0259(2)
Rb(2)	−0.4486(1)	−0.0514(1)	0.0514(1)	0.0259(2)
S(1)	−0.1242(1)	−0.0132(1)	0.2239(1)	0.0263(2)
O(1)	−0.1702(5)	0.0015(5)	0.0909(5)	0.0102(3)
O(2)	−0.0918(6)	−0.1477(4)	0.2494(6)	0.0360(12)
O(3)	−0.2228(5)	0.0342(6)	0.3126(5)	0.0326(12)
O(4)	−0.0068(6)	0.0637(6)	0.2459(6)	0.0395(14)
		(b) 120 K		
Cd(1)	0.0874(1)	0.6905(1)	.01625(1)	0.0089(1)
Cd(2)	0.4124(1)	0.5155(1)	−0.3375(1)	0.0091(1)
Cd(3)	0.1681(1)	−0.0651(1)	−0.4181(1)	0.0098(1)
Cd(4)	0.3319(1)	0.2711(1)	−0.9181(1)	0.0095(1)
Rb(1)	0.0519(1)	0.5511(1)	−0.1979(1)	0.0167(2)
Rb(2)	0.4479(1)	0.6550(1)	0.3020(1)	0.0170(2)
Rb(3)	0.1850(1)	0.2881(1)	−0.5649(1)	0.0179(2)
Rb(4)	0.3150(1)	0.9180(1)	−0.0649(1)	0.0180(1)
S(1)	0.4868(2)	0.8276(2)	0.6257(2)	0.0071(4)
S(2)	0.1243(2)	0.6160(2)	−0.5253(2)	0.0072(3)
S(3)	0.3761(2)	0.5897(2)	−0.0255(2)	0.0070(4)
S(4)	0.2246(2)	0.2273(2)	−0.2367(2)	0.0065(3)
S(5)	−0.0134(2)	0.8783(2)	−0.1261(2)	0.0067(3)
S(6)	−0.2751(2)	0.4790(2)	−0.2632(2)	0.0068(3)
O(1)	0.3293(6)	0.6082(7)	−0.1572(6)	0.0263(17)
O(2)	−0.4079(7)	0.4336(7)	−0.2440(7)	0.0265(17)
O(3)	0.5054(8)	0.6943(7)	0.5803(6)	0.0261(6)
O(4)	0.2472(8)	0.1944(8)	−0.1019(6)	0.0236(16)
O(5)	0.0050(8)	1.0107(6)	−0.0808(6)	0.0249(16)
O(6)	0.0922(6)	0.2717(7)	−0.2555(7)	0.0253(16)
O(7)	−0.1475(6)	0.8549(8)	−0.1575(7)	0.0271(17)
O(8)	0.1691(7)	0.5969(7)	−0.6589(6)	0.0230(16)
O(9)	0.2229(7)	0.5708(8)	−0.4366(6)	0.0248(16)
O(10)	0.2525(8)	0.5108(8)	−0.3984(6)	0.0298(17)
O(11)	−0.1872(6)	0.3791(7)	−0.2177(7)	0.0234(16)
O(12)	0.3525(6)	0.8500(8)	0.6582(7)	0.0294(17)
O(13)	0.2765(6)	0.6373(6)	0.0639(6)	0.0234(16)
O(14)	0.0926(7)	0.7499(7)	−0.5017(8)	0.0306(18)
O(15)	0.4076(8)	0.4548(7)	−0.0033(7)	0.0308(18)
O(16)	0.4941(8)	0.6667(7)	−0.0008(8)	0.0336(19)
O(17)	0.5631(7)	0.8519(8)	0.7444(7)	0.0319(17)
O(18)	0.2470(9)	0.1097(8)	−0.3125(9)	0.0349(19)
O(19)	0.5328(7)	0.9176(7)	0.5258(6)	0.0250(17)
O(20)	0.0331(8)	0.7902(6)	−0.0274(6)	0.0267(17)
O(21)	0.3140(6)	0.3264(7)	−0.2831(7)	0.0238(16)
O(22)	0.0064(8)	0.5400(8)	−0.5025(8)	0.0339(19)
O(23)	−0.2518(8)	0.5968(7)	−0.1880(8)	0.0338(19)
O(24)	0.0632(8)	0.8550(8)	−0.2440(7)	0.0343(19)
		(c) 85 K		
Cd(1)	0.8319(1)	0.6681(1)	0.3319(1)	0.0083(1)
Cd(2)	0.5874(1)	0.0874(1)	0.4126(1)	0.0079(2)
Rb(1)	0.8148(1)	0.3149(1)	0.1850(1)	0.0175(2)
Rb(2)	0.9480(1)	0.0520(1)	0.5519(1)	0.0153(2)
S(1)	0.9866(2)	0.2245(2)	−0.1239(2)	0.0066(5)
S(2)	0.7757(2)	0.3761(2)	0.5133(2)	0.0061(5)
S(3)	0.8759(2)	−0.0133(2)	0.2245(2)	0.0058(5)
O(1)	1.0339(7)	0.3137(6)	−0.2229(6)	0.0215(16)
O(2)	0.6863(6)	0.2762(7)	0.4653(7)	0.0220(17)
O(3)	0.7527(7)	0.4080(7)	0.6479(6)	0.0306(17)
O(4)	1.0057(7)	0.0918(6)	−0.1690(7)	0.0263(18)
O(5)	0.8528(6)	0.2475(8)	−0.0928(7)	0.0304(18)
O(6)	0.9077(7)	0.3309(7)	0.4942(7)	0.0270(17)
O(7)	0.8303(7)	0.0060(7)	0.0914(7)	0.0267(17)
O(8)	0.7771(6)	0.0346(7)	0.3138(6)	0.0224(17)
O(9)	1.0613(7)	0.2489(8)	−0.006(7)	0.0333(19)
O(10)	0.7523(9)	0.4939(7)	0.4377(7)	0.0336(19)
O(11)	0.9941(8)	0.0624(8)	0.2469(9)	0.0363(19)
O(12)	0.9074(8)	−0.1477(6)	0.2479(8)	0.0319(18)

Table 3. Bond-Valence Sums for Atoms in the Cubic (298 K), Monoclinic (120 K), and Orthorhombic (85 K) Structures of $Rb_2Cd_2(SO_4)_3$

cubic phase (298 K)		monoclinic[a] phase (120 K)		orthorhombic[a] phase (85 K)	
Rb1	0.86	Rb1	1.07	Rb1	0.87
		Rb2	1.08		
Rb2	1.03	Rb3	0.93	Rb2	1.09
		Rb4	0.88		
Cd1	2.35	Cd1	2.25	Cd1	2.39
		Cd2	2.38		
Cd2	2.26	Cd3	2.38	Cd2	2.29
		Cd4	2.38		
S	6.09	S	6.26	S	6.28
O1	1.92	O1	1.93	O1	1.92
O2	1.95	O2	1.98	O2	1.96
O3	1.88	O3	1.96	O3	1.92
O4	1.88	O4	1.94	O4	2.04

[a] For the sake of simplicity, in the monoclinic and orthorhombic structures the values given to the sulfur and the oxygen atoms have been averaged among those atoms that are symmetry-equivalent in the cubic phase.

meter with a crystal-to-detector distance of 6.03 cm. The diffraction intensities were measured with monochromated Mo Kα radiation ($\lambda = 0.7107$ Å). The reflections from 150 frames were indexed to a cubic unit cell (Table 1). The data were collected based on 4 sets of runs covering a complete sphere of reciprocal space with each set at different φ angle ($\varphi = 0°$, 90°, 180°, 270°). Each frame covered 0.3° in ω for 10-s exposure time. The data were 98.3% complete to 56° in 2θ. The details of data collection and refinement are listed in Table 1.

(b) Structure at 120 K (Monoclinic $P2_1$ Case). The crystal was cooled to 120 K (about 10 K below T_c; reported $T_c = 129$ K[16]) with an Oxford Cryosystem Nitrogen open-flow cryostat, which provides a temperature stability of ±0.05 K. At 120 K, the crystal completely transforms to a monoclinic phase. Sufficient time (1 h) was allowed for the intermediate phase to stabilize before collecting the data. Friedal equivalents were evaluated to confirm the completeness of the phase transition. There was no evidence for the presence of an intermediate triclinic phase. The data collection strategy was similar to the one measured at room temperature.

(c) Structure at 85 K (Orthorhombic $P2_12_12_1$ Case). The crystal was further cooled to 85 K (about 20 K below T_c; $T_c \sim 103$ K[16]) and was again allowed sufficient time (1 h) to stabilize in the orthorhombic phase. Several Friedal equivalents were again carefully evaluated to verify the orthorhombicity of the phase. The data collection strategy was similar to the above two cases and the details are listed in Table 1.

Structure Determination and Refinement. The crystal structures were solved based on the direct methods using the SHELXS module in the WinGX[18] suite of software. SHELXS[19] was used for structure solution and SHELXL[19] for refinement. The positions of the atoms Rb, Cd, and S were obtained initially from the E map followed by a difference Fourier synthesis which revealed the positions of all the remaining oxygen atoms in the structure. Further refinements with anisotropic thermal parameters for all atoms resulted in a final *R* value of 0.028 for 907 reflections for the room-temperature structure, 0.035 for 4998 reflections for the structure at 120 K, and 0.026 for 1586 reflections for the 85 K data, respectively. The details of the refinements are given in Table 1.

There is no indication of any disorder in any of the three phases and the structure solution is straightforward. The data sets are well-behaved and there were no lattice distortions seen. It is of interest to note that the data sets obtained for TlCdS showed variable profiles and suggested either twinning

(17) Bruker. *SMART and SAINT*; Bruker AXS Inc.: Madison, WI, 1998.
(18) Farrugia, L. J. *J. Appl. Crystallogr.* **1999**, *32*, 837.
(19) Sheldrick, G. M. *SHELXS97 and SHELXL97*; University of Göttingen: Göttingen, Germany, 1997.

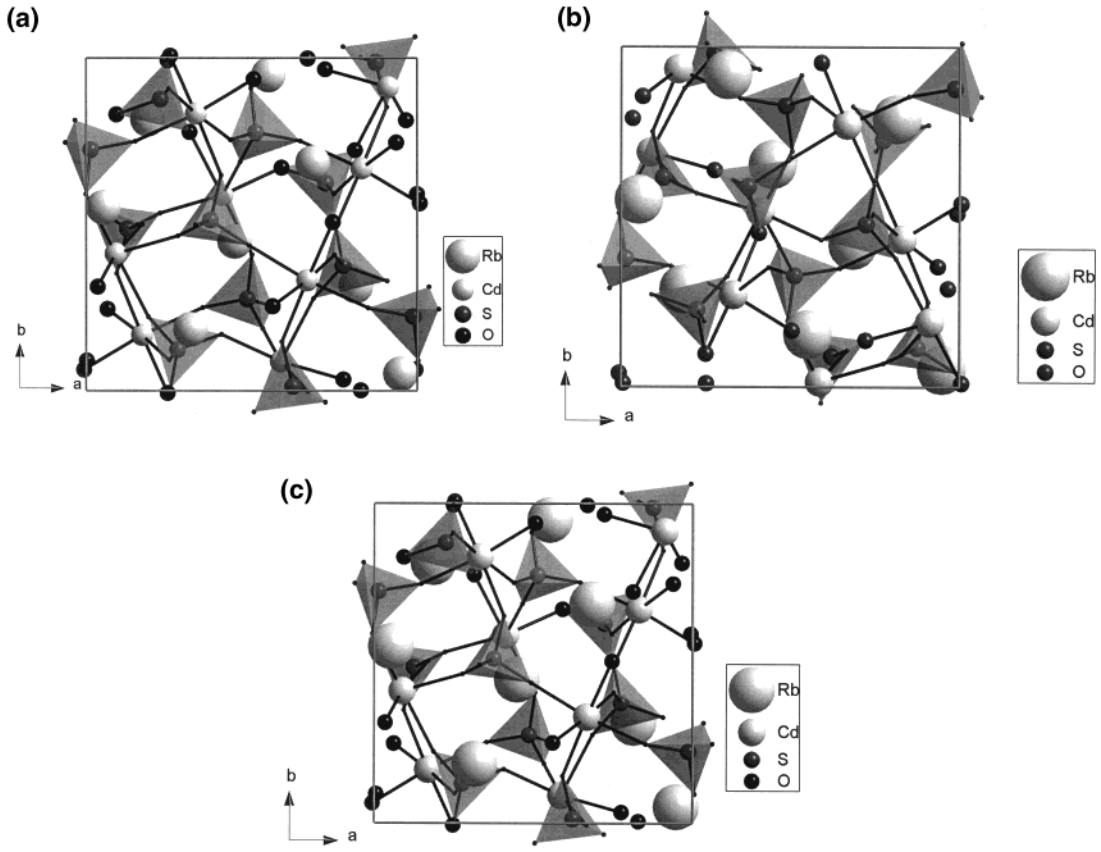

Figure 1. (a) Packing diagram of RbCdS at 298 K. (b) Packing diagram of RbCdS at 120 K. (c) Packing diagram of RbCdS at 85 K.

or the formation of an intermediate triclinic phase. The crystals of RbCdS appear to show no distortion and hence allows for the confirmation of the phase transition pathway as cubic → monoclinic → orthorhombic with no intermediate triclinic phase. The absolute configuration of the three phases was determined using the Flack parameter[20] in the SHELXL refinement strategy. The atomic coordinates along with the equivalent thermal parameters are listed in sections a, b, and c, respectively, of Table 2. PARST97[21] is used for geometrical calculations and DIAMOND[22] for drawing the packing motifs and plotting the thermal ellipsoids. Selected bond lengths and bond angles are listed in Table 4, available as Supporting Information. Table 3 lists the bond valence sums for all three phases. The packing diagrams are given in Figure 1a−c and the coordination around the Rb atoms of the three phases is shown in Figures 3a−c and 4a−c. The thermal ellipsoids for the three phases are shown in parts a−c, respectively, of Figure 2.

Results and Discussion

The structure of RbCdS, which has a transition pathway from cubic to orthorhombic via a monoclinic phase with respect to the lowering of temperature, has been studied for the first time in detail. Since the crystals are grown at elevated temperature, it is likely that lattice distortions creep in during crystallization and the earlier report[12−14] could have been a consequence of the above. However, it should be noted that all the phases generated are ferroelectric with the crystals belonging to noncentrosymmetric space groups. The possibility of an occurrence of super lattice reflections followed by lattice modulations[15] appears to be completely absent in RbCdS. The entire structural study was made on the same single crystal, to prove this point beyond doubt. Thus, we believe that RbCdS would now serve as an ideal model for the structures of type I langbeinites.

Structure at 298 K. The structure of RbCdS is isostructural with TlCdS and consists of SO_4 tetrahedra with distorted coordination polyhedra around each metal cation (Figure 1a). The cations occupy positions along the 3-fold axis with each rubidium atom nine-coordinated to the oxygen atoms. The distorted octahedra around Cd1 and Cd2 are generated through the 3-fold axis symmetry operation on independent oxygen atoms. The sulfate tetrahedra are regular with the S−O distances ranging from 1.460(5) to 1.475(6) Å, which is similar to those found in type II langbeinites. Even though an earlier study on TlCdS indicates a regular SO_4 tetrahedron,[23] the more recent study indicates distorted tetrahedra.[11] To obtain a measure of bond strengths, we have calculated the bond valence sum [24] on each atom in the unit cell and it is interesting to point out that in the current study there is no indication of the drastic underbonding on the Rb atoms and overbonding on the S atoms, as reported for the corresponding atoms in TlCdS.[11] Table 3 indicates that other than the slight underbonding on the Rb1 atom there is nothing unusual in the bonding mechanism in RbCdS. The thermal parameters of the oxygen atoms appear quite normal, suggesting that this structure is "well-ordered".

(20) Flack, H. D. *Acta Crystallogr.* **1983**, *A39*, 876.
(21) Nardelli, M. *J. Appl. Crystallogr.***1995**, *28*, 659.
(22) Pennington, W. T. *J. Appl. Crystallogr.* **1999**, *32*, 1028.
(23) Cao, H.; Dalley, N. K.; Boerio-Goates, J. *Ferroelectrics* **1993**, *146*, 45.
(24) Brown, I. D.; Alternatt, D. *Acta Crystallogr.* **1985**, *B41*, 244.

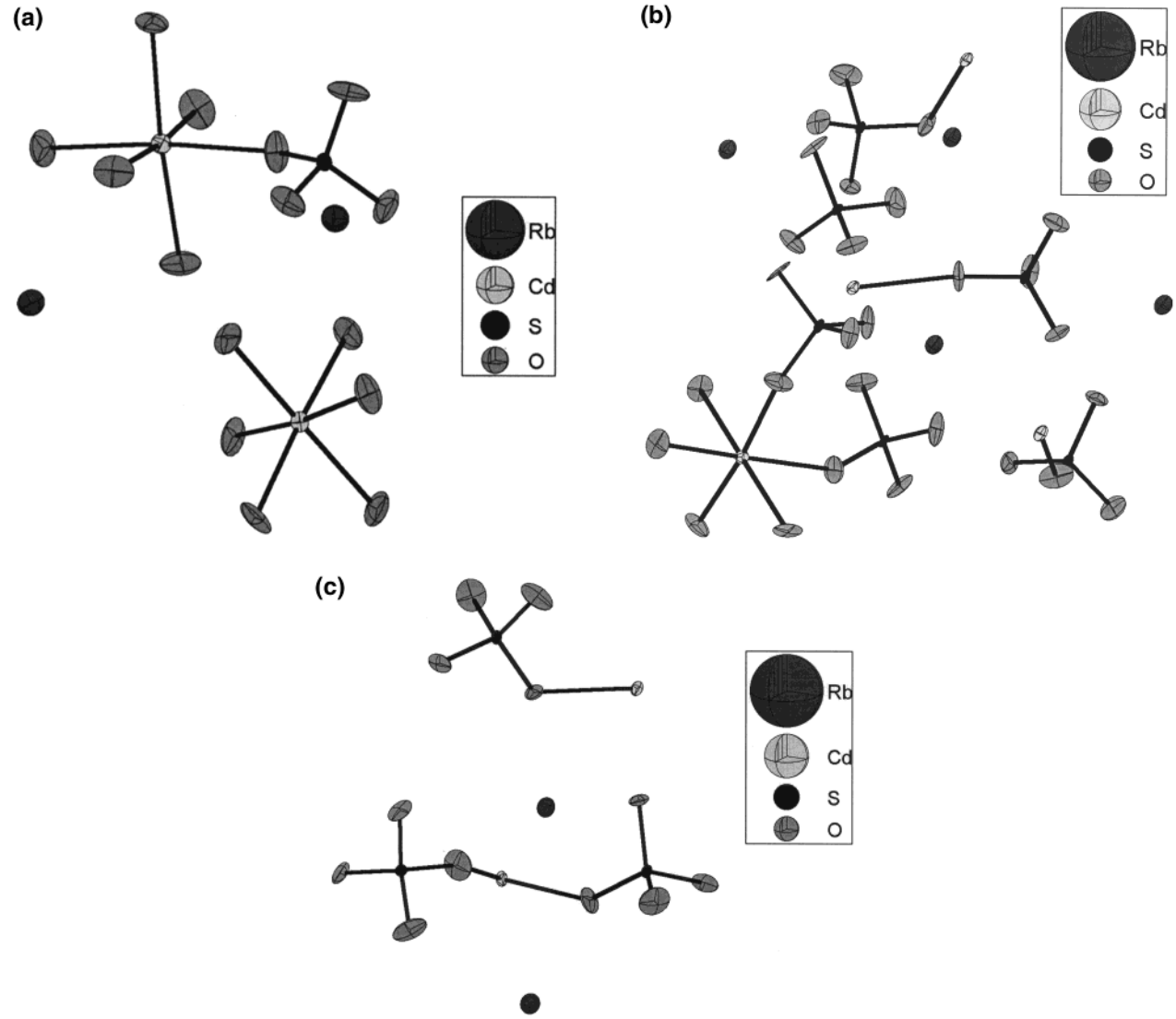

Figure 2. (a) ORTEP diagram of RbCdS at 298 K. (b) ORTEP diagram of RbCdS at 120 K. (c) ORTEP diagram of RbCdS at 85 K.

Structure at 120 K. The cell dimensions show the usual contraction expected upon cooling with slight differences in the third decimal place (Table 1) while the angle distorts by 0.025° in β. The resulting monoclinic phase thus shows very small displacements in the heavy atom positions. The SO_4 tetrahedra on an average show a slight decrease in the bond lengths with variations from 1.442(7) to 1.478(8) Å. The absence of the 3-fold axis of symmetry is evident from the nature of the metal cation coordinates. It is to be noted that no new contacts between cadmium and oxygen are observed while the Rb cations form more complicated polyhedra (Figures 3b and 4b). These small shifts in Rb positions along with the rotation in the SO_4 unit generate two different types of polyhedra at Rb sites. Rb1 is nine-coordinated to the oxygen atoms and Rb2 has a coordination number of ten. Bond valence sums also indicate that there are two types of Rb environments, one overbonded and the other underbonded. The coordination around the Cd atom, however, is retained and so the bond valence sum values are similar. The sulfur atom appears overbonded while the oxygen atoms of the SO_4 tetrahedra remain unchanged. The thermal ellipsoids (Figure 2b) do not suggest any significant distortion and the X-ray diffraction pattern has no indications of either twinning or modulation.

Structure at 85 K. The transformation from the monoclinic to the orthorhombic phase is facile. The displacement in positional coordinates of the heavy atoms from the room temperature structure to the 120 K are generally larger than the deviations observed between the cubic to orthorhombic phase at 85 K(Table 2a−c). This suggests that the orthorhombic phase is indeed a more stabilized phase at this temperature. The Friedel pair measurements evaluated give unequivocal proof on the formation of the orthorhombic phase at 85 K. The most interesting feature is that the SO_4 tetrahedra now exhibit considerable variations in S−O bond lengths with the distances ranging from 1.437(7) to 1.469(7) Å. Table 3 shows that the bond valence sums for all the atoms corresponding to the orthorhombic phase do not deviate considerably from those of the cubic and monoclinic phases. However, the effect is felt at the sulfur atom sites which overbond as the temperature is lowered. The oxygens of the SO_4 units on an average show normal distribution of bond strengths.

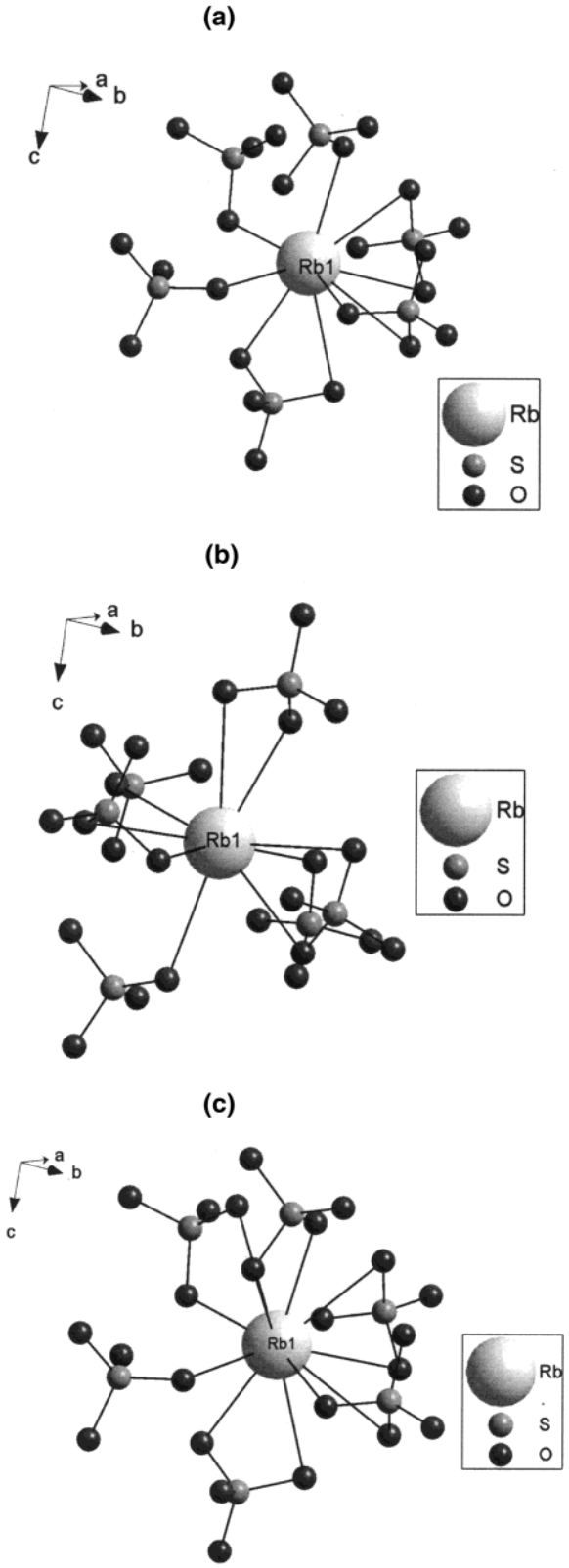

Figure 3. (a) Coordination of the Rb1 atom at 298 K. (b) Coordination of the Rb1 atom at 120 K. (c) Coordination of the Rb1 atom at 85 K.

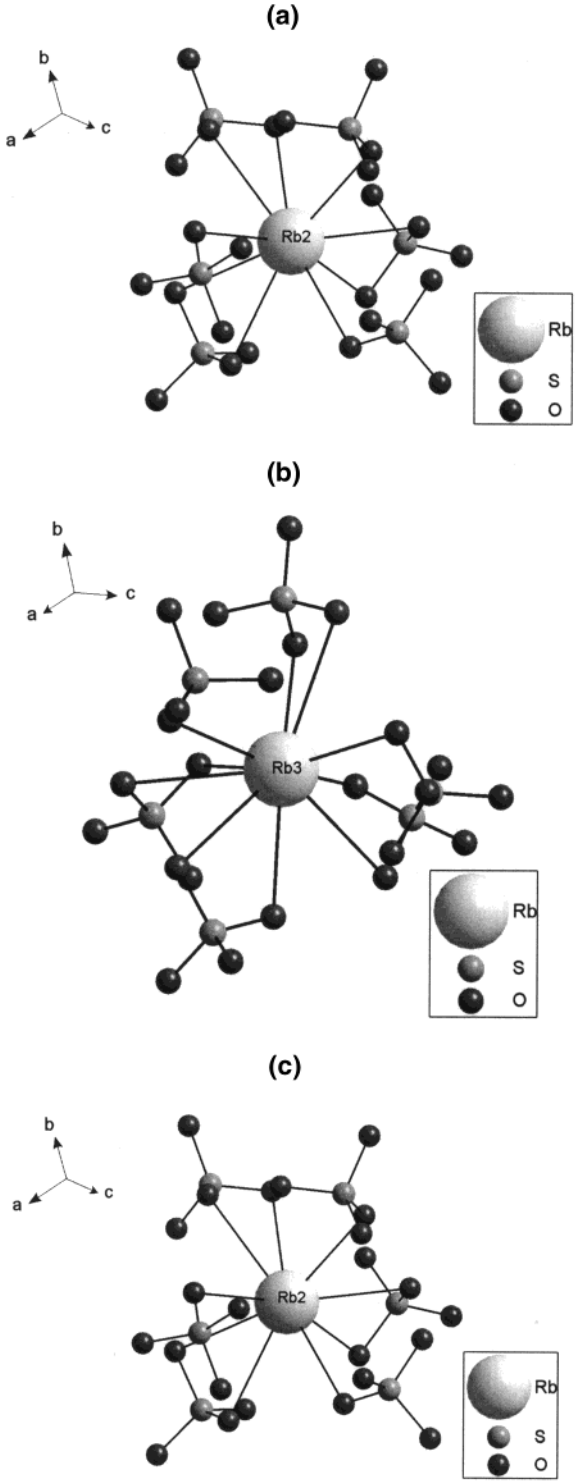

Figure 4. (a) Coordination of the Rb2 atom at 298 K. (b) Coordination of the Rb2 atom at 120 K. (c) Coordination of the Rb2 atom at 85 K.

Conclusions

We have shown that RbCdS transforms from the cubic phase at room temperature to an orthorhombic phase at 85 K through a single well-defined monoclinic phase at 120 K. This study unequivocally indicates that there is no intermediate triclinic phase for RbCdS. The accuracy in the crystal structure analysis at 12 K (GOF = 1.04; R [$I > 4\sigma$I] = 0.035; wR [$I > 4\sigma$I] = 0.083) suggests that there is no other possible phase. This is in contrast to the values observed at 121 K for TlCdS which generated the complex domain structure. We believe that TlCdS is an exception in the langbeinite type I series, which display cubic → monoclinic → orthorhombic transition. The investigation of structural changes with temperature, specially in terms of bond valence sums, point out the importance of the bonding

at the Rb sites and the subsequent rotations of the SO_4 tetrahedra to be the driving force for ferroelectric transition in RbCdS. It is conclusive thus to mention that type I langbeinites undergo a change from cubic to orthorhombic phase with lowering of temperature via an intermediate monoclinic phase.

Acknowledgment. Data collection on the DST sponsored CCD facility at the chemical sciences division IISc is acknowledged. G. Nalini thanks CSIR New Delhi for the award of a fellowship.

Supporting Information Available: DSC pattern in the range 105 K to room temperature, powder X-ray diffraction pattern of RbCdS at 298 and 120 K, and selected bond lengths and bond angles at 298,120, and 85 K are available as Supporting Information. This material is available free of charge via the Internet at http://pubs.acs.org.

Note Added after ASAP Posting

This article was released ASAP on 8/30/2002. There has been a change in authorship. The new version was posted on 9/4/2002.

CM020566H